Turbulence Spectra and Eddy Diffusivity over Forests

XUHUI LEE

School of Forestry and Environmental Studies, Yale University, New Haven, Connecticut

(Manuscript received 3 October 1995, in final form 12 February 1996)

ABSTRACT

The main objectives of this observational study are to examine the stability dependence of velocity and air temperature spectra and to employ the spectral quantities to establish relations for eddy diffusivity over forests. The datasets chosen for the analysis were collected above the Browns River forest and the Camp Borden forest over a wide range of stability conditions.

Under neutral and unstable conditions the nondimensional dissipation rate of turbulent kinetic energy (TKE) over the forests is lower than that from its Monin–Obukhov similarity (MOS) function for the smooth-wall surface layer. The agreement is somewhat better under stable conditions but a large scatter is evident. When the frequency is made nondimensional by the height of the stand (h) and the longitudinal velocity at this height (u_h), the Kaimal spectral model for neutral air describes the observations very well. The eddy diffusivity formulation $K = c\sigma_w^4/\epsilon$ provides a promising alternative to the MOS approach, where σ_w is the standard deviation of the vertical velocity and ϵ TKE dissipation rate. Current datasets yield a constant of 0.43 for c for sensible heat in neutral and stable air, a value very close to that for the smooth-wall surface layer. It is postulated that c is a conservative parameter for sensible heat in the unstable air, its value probably falling between 0.41 and 0.54. In the absence of ϵ data, it is possible to estimate K from measurements of the local mean wind u and air stability. As a special case, it is shown that $K = 0.27(uh/u_h)\sigma_w$ under neutral stability. This relation is then used to establish a profile model for wind speed and scalar concentration in the roughness sublayer. The analysis points out that u_h and h are important scaling parameters in attempts to formulate quantitative relations for turbulence over tall vegetation.

1. Introduction

Atmospheric exchange over forests is different from that in the smooth-wall surface layer in that eddies responsible for the process are a result of the dynamic coupling between the vegetation and the atmospheric flow (Hill 1989; Raupach et al. 1989). Spectral analysis is a powerful tool in revealing information about scales and patterns of such eddy motions. For example, energy containing frequencies of the velocities appear invariant with height above the canopy (Raupach et al. 1986; Kaimal and Finnigan 1994). When compared with flow over smooth surfaces, the spectra usually have a more pronounced peak (Shaw et al. 1974; Thompson 1979; Anderson et al. 1986), and tend to shift to lower frequencies when plotted against the frequency made nondimensional by the local longitudinal velocity u and distance above the displacement height z_d (Thompson 1979; Anderson et al. 1986). Most of the previous spectral analyses were performed for near-neutral air, in part because the well-defined behavior of the neutral spectra over smooth surfaces can facilitate a comparison. The first objective of this study is to examine, with use of two forest datasets covering a wide range of stability conditions, the stability dependence of spectral quantities of velocities and air temperature including the dissipation rate of turbulent kinetic energy (TKE), spectral peaks and peak frequencies, and the vertical integral scale.

A second objective is to explore the spectral quantities in the context of quantifying the vertical mixing. This is motivated by the need for predicting eddy diffusivity from knowledge of turbulence in many environmental applications and yet the traditional Monin–Obukhov similarity (MOS) approach has been problematic for flow over forests. Emphasis will be placed on the postulation that the spectral information of the vertical velocity fluctuations is sufficient for the estimate of the vertical eddy diffusivity (Hanna 1968). In addition, two other diffusivity formulations for stable air will be briefly discussed.

2. Data and analysis

a. Sites and instrumentation

Turbulence data collected at Brown River (BR) in 1990 and at Camp Borden (CB) in 1993 were chosen for the present analysis. The BR forest was documented by Lee and Black (1993) and CB forest by Neumann

Corresponding author address: Dr. Xuhui Lee, School of Forestry and Environmental Studies, Yale University, 205 Prospect Street—Sage Hall, New Haven, CT 06511.
E-mail: xhlee@minerva.cis.yale.edu

et al. (1989) and Shaw et al. (1988). Additional information on the CB experiment can be found in Lee et al. (1996). Air was extremely to moderately unstable during the BR experiment, and was moderately unstable to very stable during the CB experiment. Table 1 provides the main attributes of these two datasets. About 50 hourly runs from BR and 100 from CB made under good fetch conditions (greater than 350 m at BR and greater than 2 km at CB) were analyzed.

b. Data analysis

1) Reynolds statistics

Coordinate rotation was performed to the velocity components following the procedure of Tanner and Thurtell (1969). Reynolds statistics were calculated over hourly intervals. Stability parameter was calculated from kinematic sensible heat flux and friction velocity as

$$\xi = -\frac{(g/\bar{T})\overline{w'T'}}{u_*^3/(kz_d)},$$

where k (=0.4) is the von Kármán constant, g gravitational acceleration, $\bar{T}$ mean air temperature in kelvins, $\overline{w'T'}$ kinematic sensible heat flux, and u_* friction velocity. The displacement height is taken as $0.7h$. Local flux values are used here and later in the construction of the MOS functions, a practice implying local scaling under stable conditions (Nieuwstadt 1984).

Two parameters, height of the stand (h) and mean longitudinal velocity at this height (u_h), are important scaling dimensions in the present study. For purposes of discussion we shall loosely refer to the scaling scheme involving h and u_h as canopy scaling. Parameter u_h at CB was approximated by wind speed at z = 22.4 m. At the BR site, direct measurements of u_h were available for 25% of the runs. For the remaining runs, u_h was calculated from the wind speed provided by a sensitive cup anemometer at $z = h$. This involves regression of cup wind speed against direct measurements of u_h and application of the regression equation for runs without direct u_h measurements. It was found that unit ATI-V noticeably underestimated the mean longitudinal velocity because of the aerodynamic shadow effect. Corrections were therefore made based on field comparisons with the other two units. Other quantities with ATI-V such as velocity and temperature variances, friction velocity, and TKE dissipation rate were not affected (Lee et al. 1996).

2) Eddy diffusivity for sensible heat

Concurrent observations of the temperature profile were made at CB for about 25 nighttime runs (stable air). Eddy diffusivity for sensible heat (K_h) at z = 34.5 m was determined from $K_h = -\overline{w'T'}(\partial\theta/\partial z)^{-1}$, where the potential temperature gradient $\partial\theta/\partial z$ was determined from temperature measured with ventilated platinum resistance thermometers at z = 43.4 and 25.7 m. To increase the sample size, we resorted to wind data for neutral air ($|\xi| < 0.06$) such that $K_h = -(\overline{u'w'})_m(\partial u/\partial z)^{-1}$, where $\partial u/\partial z$ is the longitudinal velocity gradient between z = 34.5 and 22.4 m, $-(\overline{u'w'})_m$ momentum flux averaged over the two heights, and equality of diffusivities of heat and momentum is assumed. The diffusivity determined as such is for the algebraic mean height z = 28.5 m.

3) Spectral analysis

Hourly time series of the longitudinal (u) and vertical (w) velocity components and air temperature (T) were broken into 12 equal segments. Discrete Fourier transformation was applied to each segment and composite spectra and cospectra were formed for each hour. Signals were detrended and tapered with a Hanning window prior to the transformation. Power spectrum of quantity $x(S_x)$ is defined such that

$$\sigma_x^2 = \int_0^\infty S_x df,$$

where σ_x is the standard deviation of x and f (Hz) natural frequency. In general the integrated spectral or cospectral energy agrees well with the corresponding Reynolds statistics. Cospectra of the time series display considerable noise in the high-frequency range and will not be presented in this paper.

Wavelike events were very common at CB at night. Their existence is evident from either a broadened en-

TABLE 1. Main attributes of the turbulence datasets.

Site	h (m)	z (m)	Sensor type	Pathlength (cm)	Sampling rate (Hz)
BR	16.7	16.7	3D sonic anemometer/thermometer (ATI-V)	10	9.9
		23.0	3D sonic anemometer/thermocouple (ATI-B)	25	9.9
CB	20.0	22.4	3D sonic anemometer/thermometer (ATI-V)	10	10.0
		34.5	3D sonic anemometer/thermometer (SOLENT-A)	15	20.8

Note: ATI-V: model SWS-211/3V, Applied Technologies Inc., Boulder, Colorado; ATV-B: model BH-478B/3, Applied Technologies Inc.; SOLENT-A: model 1012R2A, Gill Instruments, Lymington, England.

ergy-containing range of the w spectrum or the presence of a wave frequency at all three (u, w, and T) spectra in addition to the regular peaks due to turbulent motions. The wavelike motion acted to enhance cogradient fluxes or to create countergradient fluxes in a somewhat unpredictable manner (Lee et al. 1996), rendering the stability parameter ξ inappropriate. To avoid unnecessary complications, we have excluded these wavelike events from the present discussion.

4) TKE DISSIPATION RATE

The spectra of u and w have the following form in the inertial subrange

$$fS_u = \alpha_u \epsilon^{2/3} \left(\frac{f}{u}\right)^{-2/3}, \quad (1)$$

$$fS_w = \alpha_w \epsilon^{2/3} \left(\frac{f}{u}\right)^{-2/3}, \quad (2)$$

where α_u (=0.15) and α_w (=4/3α_u) are the Kolmogorov constants (Panofsky and Dutton 1984), u mean longitudinal velocity, and ϵ is TKE dissipation rate. Equation (1) is employed to estimate ϵ from the energy spectrum in the frequency range defined by a procedure described below.

Both theoretical analyses (Kaimal et al. 1968; Silverman 1968; Kristensen and Fitzjarrald 1984) and experimental investigations (e.g., Anderson et al. 1986) show that the velocity spectra will have a rapid rolloff at the high-frequency end due to spatial averaging along the anemometer path. Using the work of Kaimal et al. (1968) as a rough guide, we have chosen $f_{max} = u/4\pi d$ as the upper-frequency limit, below which the effect of spatial averaging is negligible, where d is the sonic anemometer pathlength (Table 1). The lower-frequency limit f_{min}, which defines the beginning of the inertial subrange, was determined in a more ad hoc manner. The u spectrum was first graphed for all runs. The two-thirds law was then examined for each run. It is found that the 2/3 slope was established for frequencies greater than $0.2u/z_d$ and u/z_d for BR and CB, respectively. These were then used as f_{min}. The estimate of ϵ was made from the spectral energy of u over $f_{min} < f < f_{max}$.

The fact that the 2/3 slope is lost at frequencies beyond f_{max} raises the question of whether there is any need for rapid sampling with sonic anemometers. It is shown that ϵ can also be determined from the u time derivative (see appendix). The success of this method requires a sufficiently high sampling rate. Although this rate exceeds the capacity of current commercial sonic anemometers that we are aware of, it is possible that some future design can meet the requirement.

3. Results and discussion

a. TKE dissipation

Figure 1 compares the MOS function for ϵ over forests with those established for smooth surfaces as

$$\phi_\epsilon = 1 - \xi \quad (\xi \leq 0), \quad (3)$$

$$\phi_\epsilon = 1 + 5\xi \quad (\xi > 0), \quad (4)$$

(Panofsky and Dutton 1984; Kaimal and Finnigan 1994), where ϕ_ϵ is defined as $\phi_\epsilon = kz_d\epsilon/u_*^3$. The data presented here appear to be the first of their kind relating ϵ over forests to air stability. There is a rapid increase in ϕ_ϵ as air becomes increasingly stratified. The observation under stable conditions appears to follow Eq. (4), although a large scatter is evident. Under unstable conditions, the observed values are generally lower than those predicted from Eq. (3). Data from z = 16.7 m (top of the stand) at BR and those from CB, obtained under moderate instability, deviate noticeably from those obtained at z = 23.0 m at BR, which constitute the main body of data points over $\xi < 0$. The averaged values at near neutrality ($|\xi| < 0.06$) were 0.73 and 1.09 near the treetops (z = 22.4 m) and above the stand (z = 34.5 m), respectively, at CB. Values less than unity were also observed at a boreal black spruce forest (0.45 averaged over $-0.03 < \xi < 0$; P. Frenzen and C. Vogel 1995, personal communication).

Reasons for the disparity at neutrality will become clear with the help of the budget equation of TKE over a horizontally homogeneous surface

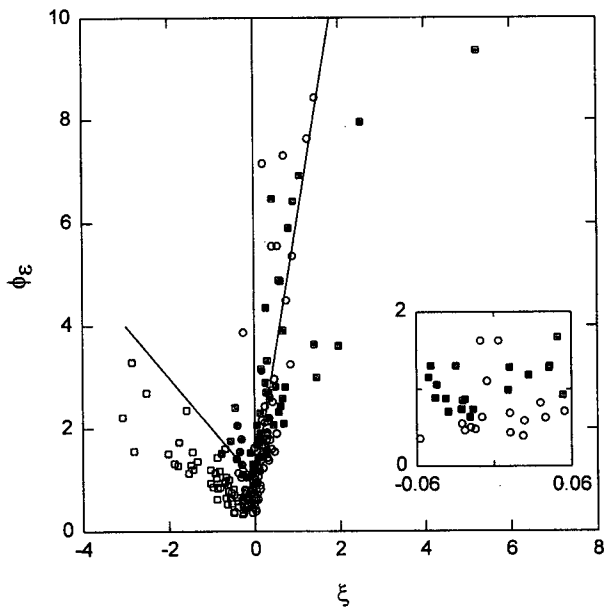

FIG. 1. MOS function for TKE dissipation: open square, z = 23.0 m (BR); solid circle, z = 16.7 m (BR); solid square, z = 34.5 m (CB); open circle, z = 22.4 m (CB); line, Eqs. (3) and (4). The insert is for runs made under near-neutral stability ($|\xi| < 0.06$).

$$\frac{\partial \bar{e}}{\partial t} = u_*^2\left(\frac{\partial u}{\partial z}\right) + \frac{g}{T}(\overline{w'T'}) - \frac{1}{\rho}\frac{\partial}{\partial z}(\overline{w'p'}) - \frac{\partial}{\partial z}(\overline{ew'}) - \epsilon, \quad (5)$$

where the notation is conventional. Assuming steady state and neutral stability and ignoring the pressure transport, one can arrange Eq. (5) to give

$$\phi_\epsilon = \frac{kz_d}{u_*}\frac{\partial u}{\partial z} - \frac{kz_d}{u_*^3}\frac{\partial}{\partial z}(\overline{ew'}). \quad (6)$$

The profile model developed later shows that wind speed in the roughness sublayer is parabolic rather than logarithmic with height. In other words the first term on the rhs of Eq. (6) should be less than one. The second term (the transport term) is generally thought to be negligible over a smooth surface (e.g., Wyngaard and Coté 1971), although Högström (1990) reported data that indicate the contrary. Over a vegetated surface, turbulent transport would export TKE upward at a rate of about 20%–80% of its production (Raupach et al. 1986; Wilson and Shaw 1977; Leclerc et al. 1990; Meyers and Baldocchi 1991) so that the derivative $\partial(\overline{ew'})/\partial z$ is always positive. Both mechanisms will cause the conventionally defined ϕ_ϵ to be less than unity. Indeed there is no reason to believe that a universal form of ϕ_ϵ exists over forests.

b. *Spectral features*

1) Spectra under neutral stability

We begin by presenting three sets of spectra observed under neutral stability (Fig. 2). Mean statistics for the period chosen for analysis are given in Table 2. For comparison, we have also plotted the relations established from the Kansas experiment (e.g., Kaimal and Finnigan 1994; Kaimal et al. 1972)

$$\frac{fS_u}{u_*^2} = \frac{102n}{(1 + 33n)^{5/3}}, \quad (7)$$

$$\frac{fS_w}{u_*^2} = \frac{2.1n}{1 + 5.3n^{5/3}}, \quad (8)$$

$$\frac{fS_T}{T_*^2} = \begin{cases} \dfrac{80.1n}{(1 + 24n)^{5/3}}, & n \leq 0.15 \\ \dfrac{36.6n}{(1 + 12.5n)^{5/3}}, & n > 0.15, \end{cases} \quad (9)$$

but with the reduced frequency defined as $n = fh/u_h$. While Eqs. (7) and (8) are the original relations, Eq. (9) has been scaled by a factor of 1.5 in order to produce a match between its integral and the observed ratio σ_T^2/T_*^2. The canopy scaling has collapsed all three spectra remarkably well. If the conventional reduced frequency fz_d/u had been used, we would have seen the peaks shift to lower frequencies in comparison with the Kaimal model, the shift being most obvious for the w spectrum and at heights near the treetops. This phenomenon was noted by Anderson et al. (1986) and others. The modified Kaimal relations agree well with observations except for a few minor discrepancies: the w spectral peak is sharper than that calculated with Eq. (8). At the low-frequency end, the observed u and T spectra display a quicker rolloff, which we suspect was an artifact caused by the truncation of the original time series. These disparities are inconsequential in terms of engineering applications.

The spatial averaging along the path of sonic anemometers resulted in a rolloff faster than the $^2/_3$ slope at the high-frequency end of the u and w spectra. The high-frequency part of the T spectrum is much noisier than the velocity spectra, a portion of which (toward the high-frequency end) displays a slightly positive slope, probably a result of the aliasing effect. This problem is common to all the three fast-response units and because of this, no attempt was made to evaluate the dissipation rate of the T variance.

According to Eqs. (7)–(9), the peak frequencies (n_m) for u, w, and T are, in order, 0.045, 0.47, and 0.063. Adopting the view that energy containing eddies responsible for the vertical mixing advect at speed u_h, we can express their wavelength as

$$\lambda_m = \frac{f_m}{u_h} = 2.13h.$$

The invariance of the scaled peak frequency with height is observed in almost all of the reliable datasets reported in the literature. See Kaimal and Finnigan (1994) for a detailed review. It is reasonable to expect the roughness sublayer spectra to match their inertial sublayer counterparts at some height above the stand. Simple calculations involving a logarithmic wind profile indicate that the matching will occur at $z \approx 2.8$ h, at which height n_m would be the same as the spectral peak position in the scaled frequency fz_d/u. This critical height can be regarded in the spectral sense as the top of the roughness sublayer within which MOS is inadequate. Over a tall forest (e.g., $h = 20$ m), there is little hope that a constant flux layer can establish beyond this height. The general validity of MOS is therefore in serious doubt. Even if a constant flux layer does exist, it is unlikely that the theory could offer help to experimentalists as they are often forced to operate below the critical height because of the limited fetch of the site or the prohibiting cost in erecting a tall tower.

2) Spectral peaks

The normalized spectral peak for w is presented in Fig. 3 along with the smooth-wall relation represented by Dutton et al. (see Panofsky and Dutton 1984). The MOS scaling appears to collapse the w data reasonably well. Data at BR (Lee and Black 1993) and CB showed

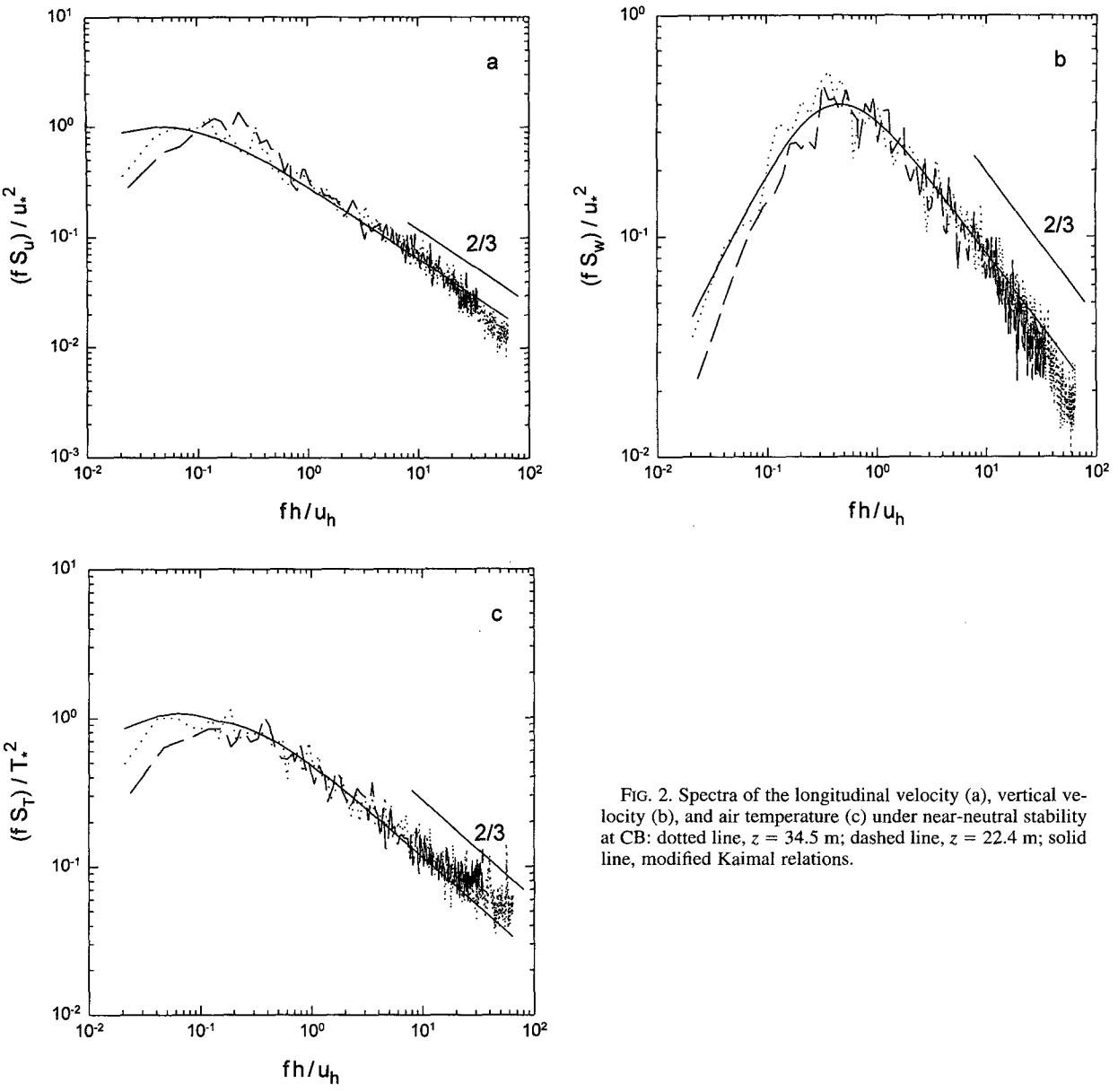

FIG. 2. Spectra of the longitudinal velocity (a), vertical velocity (b), and air temperature (c) under near-neutral stability at CB: dotted line, $z = 34.5$ m; dashed line, $z = 22.4$ m; solid line, modified Kaimal relations.

that the ratio of the w standard deviation to the friction velocity (σ_w/u_*), or the integrated spectral energy, follows closely its MOS function for smooth surfaces. So the comparison with the smooth-wall relation here serves as a simple indication of the peakness of the spectral curve. Previous analyses performed for near-neutral and slightly unstable conditions reveal that the w spectrum is more sharply peaked than that in the smooth-wall surface layer (Shaw et al. 1974; Thompson 1979; Anderson et al. 1986; see also Fig. 2c). The data in Fig. 3 indicates that this feature is in fact common under all stability conditions. The deviation from the smooth-wall relation becomes larger as the degree of stratification increases. One might attempt to associate this feature with coherent ramp structures over forests (Thompson 1979). The energy contained in the ramp motions, however, cannot account for the sharp peak because ramp structures occur at a frequency much lower than the energy containing frequency of the w spectrum. For example, data of Paw U et al. (1992) at high winds, presumably collected under near neutrality, suggest the normalized ramp frequency ($f_r h/u_h$) to be about 0.025, which is more than one decade lower than the peak frequency of the w spectrum (Fig. 2c). Shaw et al. (1974) offered a more plausible explanation: The sharp peak might be a result of turbulent wakes generated by tree crowns.

TABLE 2. Mean statistics at CB for the period 1400–1700 EDT 24 August 1993.

z = 22.4 m		
u = 3.12 m s^{-1}	u_* = 0.95 m s^{-1}	$\overline{w'T'}$ = 0.146 (m °C) s^{-1}
ϵ = 0.125 m^2 s^{-3}	σ_w = 1.09 m s^{-1}	ξ = −0.018
σ_T = 0.367°C	T_* = −0.153°C	
z = 34.5 m		
u = 4.88 m s^{-1}	u_* = 1.07 m s^{-1}	$\overline{w'T'}$ = 0.153 (m °C) s^{-1}
ϵ = 0.117 m^2 s^{-3}	σ_w = 1.34 m s^{-1}	ξ = −0.033
σ_T = 0.503°C	T_* = −0.142°C	

The following formula provides a good fit to the w data:

$$\left(\frac{fS_w}{u_*^2}\right)_{\max} = \begin{cases} 0.60 - 0.75\xi, & \xi \le 0, \\ 0.60 + 0.40\xi, & \xi > 0. \end{cases} \quad (10)$$

Note that Eq. (10) does not satisfy either the free convection or the z-less limit.

The short time window (5 min) used in the Fourier transformation prevents an examination of the u and T spectral peaks for $\xi < 0$. The data for $\xi > 0$ do not suggest a strong stability dependence, providing an average of 2.41 (standard deviation 1.46, number of runs 105) for the normalized u peak and 2.98 (2.78, 88) for the T peak, the latter being made nondimensional by $T_* = -\overline{w'T'}/u_*$.

3) PEAK FREQUENCIES

Figure 4 presents the w spectral peak frequency, made nondimensional with the canopy scaling, as a function of air stability. The scatter is due in large part to the difficulty in defining the spectral peak position. In the present analysis, the spectral peak value was determined by a single data point having maximum energy, its position being used as the peak frequency. This procedure is accurate in finding the maximum value but is prone to error in finding its position because of the flatness of the turbulence spectra. Bearing this in mind, it is fair to say that the canopy scaling has collapsed the data reasonably well. The onset of stability has brought about an abrupt change in n_m and from there on there is a clear trend with stability. Four data points observed under very stable conditions deviate from this trend, suggesting interference by weak wave activities or the possibility that the boundary layer is not fully turbulent. The reduced peak frequency is much higher than its counterpart over a smooth surface (e.g., Kaimal and Finnigan 1994) under stable conditions. Under neutral and unstable conditions the difference is not as large. The following relations are constructed to fit the data in Fig. 4:

$$n_m = \begin{cases} \dfrac{0.47}{1 - 0.52\xi}, & \xi \le 0, \\ 0.47 + 3.3\xi, & \xi > 0. \end{cases} \quad (11)$$

Once again, the reduced u and T peak frequencies are essentially invariant with $\xi(\xi > 0)$. The average values (standard deviations) were 0.31 (0.33) and 0.37 (0.22) for u and T, respectively.

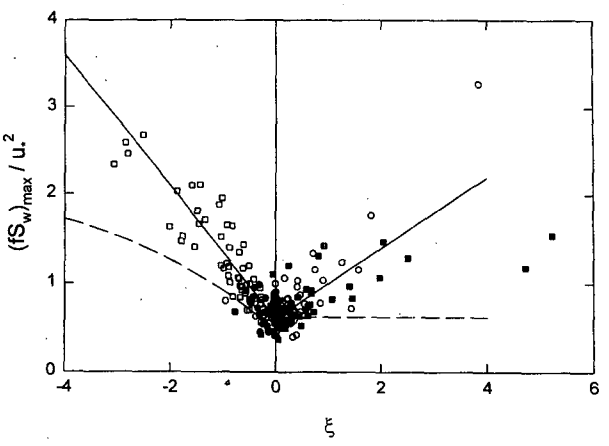

FIG. 3. Normalized w spectral peak: solid line, regression [Eq. (10)]; dashed line, relation for the smooth-wall surface layer (Dutton et al.). Other symbols as in Fig. 1.

c. Eddy diffusivity

1) HANNA'S FORMULATION

Hanna (1968) reasoned that the vertical eddy diffusivity of the atmosphere must be dependent upon the gross characteristics of the vertical velocity component of turbulent eddies. He hypothesized that the diffusivity K can be derived from spectral features of the vertical

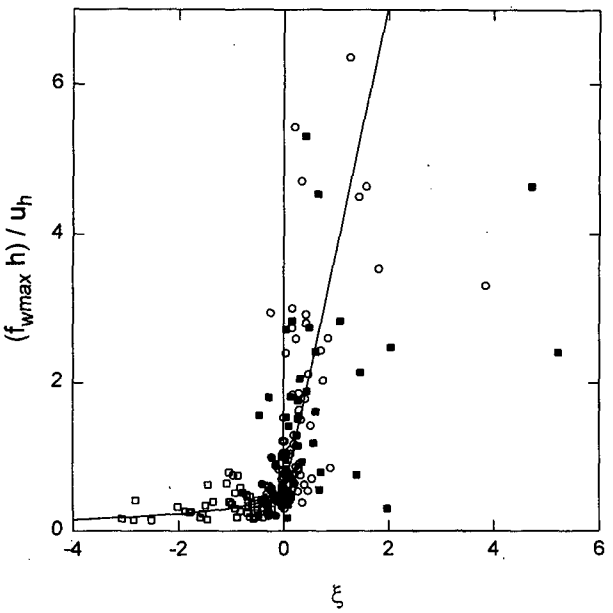

FIG. 4. Scaled spectral peak frequency for w: solid line, regression [Eq. (11)]. Other symbols as in Fig. 1.

velocity component. Specifically K may be expressed in any of the forms: $K = a_1\sigma_w\lambda_m$, $K = b_1(\epsilon\lambda_m^4)^{1/3}$, and $K = c\sigma_w^4/\epsilon$. The last relation can also be written as

$$K = cl_w\sigma_w, \tag{12}$$

where the vertical integral scale is

$$l_w = \frac{\sigma_w^3}{\epsilon}. \tag{13}$$

The scale l_w is a measure of the vertical size of those eddies responsible for most of the mixing (Tennekes and Lumley 1972). Equation (12) is essentially analogous to the Prandtl mixing length parameterization. The most important feature of Hanna's postulation is that it completely avoids the need for the MOS functions in computing the eddy diffusivity and is therefore particularly attractive in studies of flow over forests.

In his application, Hanna (1968) proposed that the proportionality coefficient c is a constant for momentum flux ($c = 0.30$) but is a function of Richardson number for heat flux. In fact, the MOS functions, which were not available at the time of his publication, can be used to investigate the stability dependence. A little manipulation of their definitions leads to

$$c = \frac{\phi_\epsilon}{\phi_h\phi_w^4},$$

for sensible heat flux and

$$c = \frac{\phi_\epsilon}{\phi_m\phi_w^4},$$

for momentum flux. The result is illustrated in Fig. 5, where we have used the empirical MOS functions for ϵ [Eqs. (3) and (4)] and

$$\phi_w = \begin{cases} 1.25(1 - 3\xi)^{1/3}, & \xi \leq 0, \\ 1.25, & \xi > 0, \end{cases} \tag{14}$$

for the w standard deviation,

$$\phi_h = \begin{cases} (1 - 16\xi)^{-1/2}, & \xi \leq 0, \\ 1 + 5\xi, & \xi > 0, \end{cases} \tag{15}$$

for temperature gradient, and

$$\phi_m = \begin{cases} \phi_h^{1/2}, & \xi \leq 0, \\ \phi_h, & \xi > 0, \end{cases} \tag{16}$$

for momentum flux (e.g., Panofsky et al. 1977; Businger et al. 1971; Dyer 1974). Also included in Fig. 5 is the result based on the local similarity theory of Nieuwstadt (1984). The neutral value of c is equal to 0.41 for both momentum and heat. For stable air, both MOS and the local similarity indicate that c is insensitive to ξ, and the same value of 0.41 can be used as an excellent approximation. The c value for sensible heat shows an abrupt increase as ξ becomes slightly negative; beyond $\xi = -0.1$, it approaches a constant of about 0.54. The c value for momentum decreases monotonically as ξ becomes increasingly negative, which is contrary to Hanna's earlier assessment. Alternatively, one may interpret the value of 0.30 he obtained as an average over the stability range of his datasets.

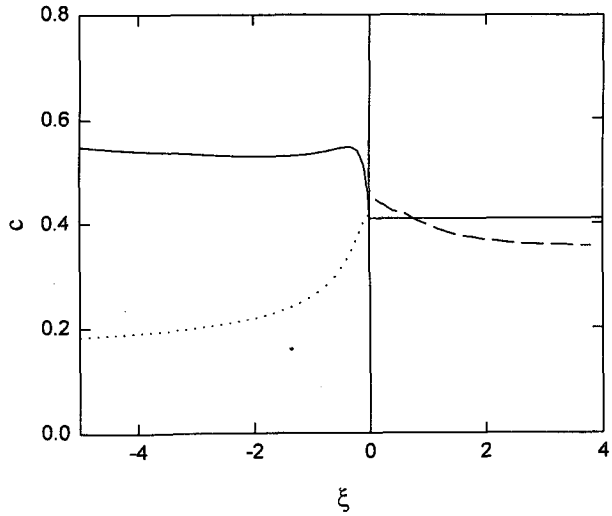

FIG. 5. The proportionality parameter c in Eq. (12) as a function of stability for flow over smooth surfaces for scalar flux (solid line) and momentum flux (dotted line) based on the surface layer MOS functions and scalar flux (dashed line) evaluated from the local similarity of Nieuwstadt (1984).

Before ending this section, a few comments on Eq. (12) and the $E-\epsilon$ closure are appropriate. Equation (12) is similar in form to the parameterization

$$K = \frac{c_\epsilon \bar{e}^2}{\epsilon}, \tag{17}$$

where the value of 0.09 is commonly adopted for the coefficient c_ϵ (Stull 1988). Using the ratio $\sigma_w^2/\bar{e} \approx 0.28$ observed in the neutral atmosphere (Panofsky and Dutton 1984), Eq. (17) suggests $c \approx 1.12$, which is obviously too high in comparison with observations.

2) K_h OVER FORESTS

Figure 6 compares K_h from Eqs. (12) and (13) and that measured over the CB forest. For runs under stable conditions σ_w and ϵ measured at $z = 34.5$ m were used in the comparison and for runs under near-neutral conditions, values averaged over two heights ($z = 34.5$ and 22.4 m) were used. Linear regression of the data in Fig. 6 yields a value of 0.43 for c, which differs only slightly from its smooth-wall value. This indicates that c is insensitive to the surface roughness. Furthermore, the plot of c against ξ for individual runs does not seem to reveal a stability dependence (Fig. 7), suggesting

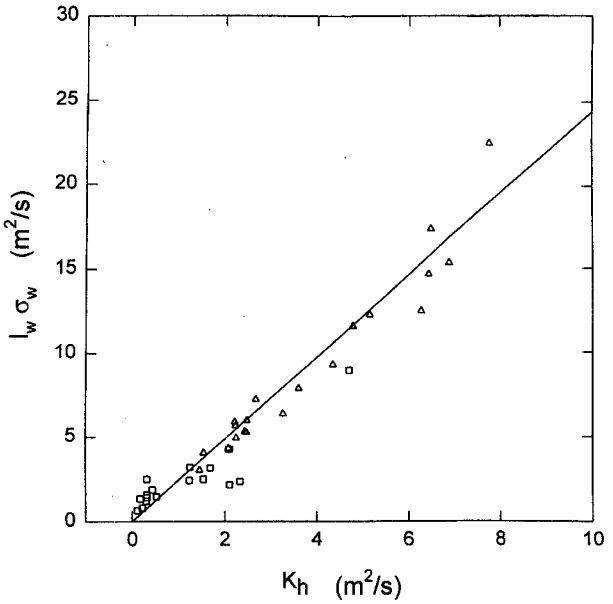

FIG. 6. Product of the vertical integral scale and the standard deviation of the vertical velocity against the measured eddy diffusivity for heat over the CB forest: open square, stable conditions; triangle, neutral stability ($|\xi| < 0.06$); line, Eq. (12) with $c = 0.41$.

that c is a parameter insensitive to air stability as well (at least for neutral and stable air). Note that most of the scatter in Fig. 7 can be explained by the small number division involved in calculating c.

So far the question remains open as to whether c is a constant for scalar flux in unstable air. One might speculate that c would increase as ξ becomes more negative. As instability increases, buoyancy feeds mean kinetic energy directly into the vertical component of TKE. This is manifested by the presence of thermals, eddies which transport heat and masses much more effectively than momentum. Because thermals are of large scale, one expects the vertical integral scale l_w to increase rapidly with instability. This is clearly evident from the data in Fig. 8. Here l_w is made nondimensional by uh/u_h, which will be shown to represent the integral scale at neutral stability. Additional evidence can be found in Fitzjarrald et al. (1988). The increase in mixing efficiency with instability is fully reflected by the increase in both the eddy size (l_w) and the intensity of the vertical motion (σ_w), without the need to increase c substantially. It seems therefore safe to postulate that c is a conservative parameter, its value probably falling between 0.41 and 0.54. This is certainly in accord with observations over smooth surfaces (Fig. 5). It is also consistent with the hypothesis that the w spectrum should contain sufficient information needed for assessing the mixing efficiency owing to turbulent motions.

The regression of the data in Fig. 8 gives

$$\frac{l_w}{(uh/u_h)} = \begin{cases} 0.65 - 0.85\xi, & \xi \leq 0, \\ \dfrac{0.65}{1 + 5.1\xi}, & 0 < \xi \leq 1, \\ 0.11, & \xi > 1. \end{cases} \quad (18)$$

In situations where no ϵ data are available, Eqs. (12) and (18) may provide a practical means of estimating the eddy diffusivity from simple measurements of local mean wind, air stability, and the vertical velocity fluctuations.

3) PROFILES IN THE ROUGHNESS SUBLAYER UNDER NEUTRAL STABILITY

Eliminating S_w from Eqs. (2) and (8) yields a solution for ϵ. Replacing ϵ in Eq. (13) with this solution, we obtain

$$l_w = 0.36\left(\frac{\sigma_w}{u_*}\right)^3 \frac{uh}{u_h} \approx \frac{0.65uh}{u_h}. \quad (19)$$

This equation reinforces the notion that eddies responsible for vertical mixing are comparable in size to the canopy height. Substituting Eq. (19) into Eq. (12) gives a new eddy diffusivity formula for neutral air over forests

$$K = \alpha\left(\frac{uh}{u_h}\right)\sigma_w, \quad (20)$$

where $\alpha = 0.27$. Equations (12), (13), and (19) suggest the properties $\epsilon \sim 1/u$ and $K \sim u$, and the height dependence of ϵ and K is no longer explicit. A com-

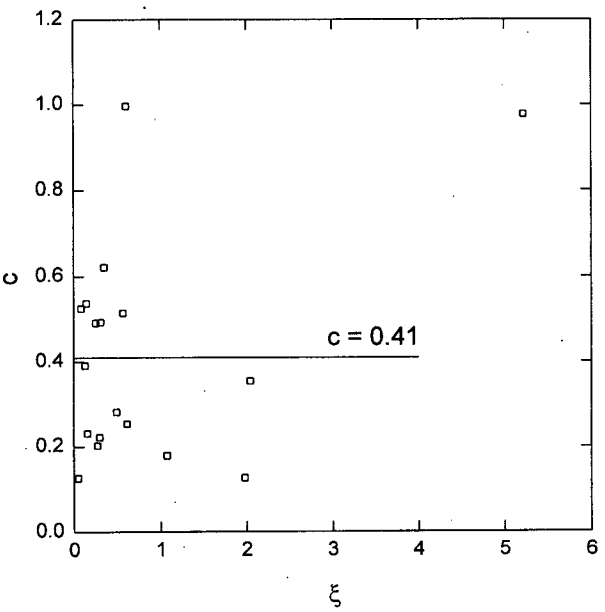

FIG. 7. Coefficient c in Eq. (12) as a function of air stability over the CB forest.

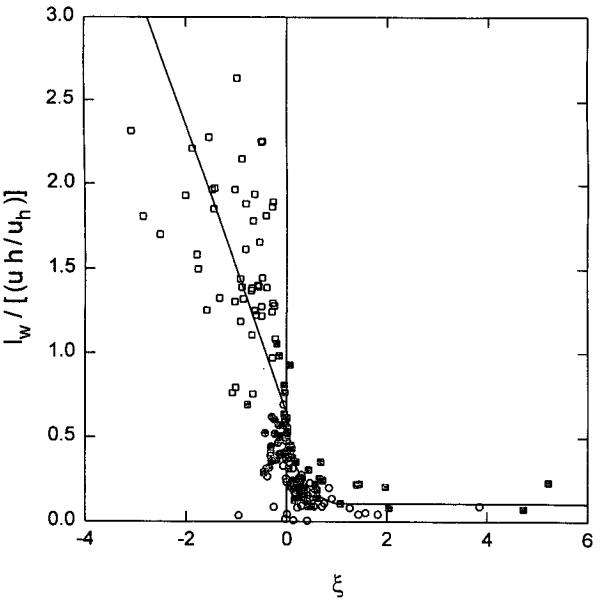

FIG. 8. Nondimensional vertical integral scale as a function of stability: line regression [Eq. (18)]. Other symbols as in Fig. 1.

parison of calculations with Eqs. (12), (13) and those with Eq. (20) is presented in Fig. (9). Equation (20) collapses well the observations at two heights, demonstrating the internal consistency of the canopy scaling. The narrow range about the 1:1 line where the data points fall indicates that the modified Kaimal relation [Eq. (8)] is a good model for the w spectrum over forests, although a slight adjustment of its coefficients may result in a better agreement in Fig. 9.

It can be shown from flux-gradient relations and Eq. (20) that

$$\frac{u}{u_*} = \left(\frac{2a}{\alpha}\frac{z-h}{h} + a^2b^2\right)^{1/2}, \qquad (21)$$

for wind speed, and

$$\frac{q-q_h}{q_*} = \left(\frac{2a}{\alpha}\frac{z-h}{h} + a^2b^2\right)^{1/2} - ab, \qquad (22)$$

for scalar concentration q, where a $(=u_h/\sigma_w)$ is the inverse of the vertical turbulence intensity on the top of the stand, $b = \sigma_w/u_*$, $q_* = -\overline{w'q'}/u_*$, and q_h scalar concentration at the treetops. Note that the two familiar surface parameters, displacement height and roughness length, do not appear in these relations. The CB dataset gives $a = 3.20$ and $b = 1.22$. While the value of b can be regarded as a universal constant, a is a parameter that depends on foliage density and plant morphology. A review of the literature shows that a is mostly in the range 2.7–3.3 (e.g., Raupach et al. 1986; Wilson et al. 1982; Gardiner 1994; Amiro and Davis 1988; Shaw et al. 1988).

Figure 10 compares the two profiles with the conventional logarithmic forms. Below the height of about $2h$, the slope of the new profiles is smaller than that of the logarithmic forms. Because the derivatives of wind speed and the scalar concentration are inversely proportional to the eddy diffusivity, an alternative interpretation of the difference is that the eddy diffusivity is "enhanced" in comparison to $K = ku_*z_d$, the relation pertaining to the smooth-wall surface layer. The degree of enhancement will obviously depend on the distance from the stand as well as stand density.

The features captured by Eqs. (21) and (22) compare favorably with observations. For example, Chen and Schwerdtfeger (1989) reported that the shapes of their observed profiles of both wind speed and temperature over a bushland were more uniform than those predicted from the logarithmic model. In a study of the flux-gradient relationships, Högström et al. (1989) found that ratios of the nondimensional gradients of wind speed and temperature to their corresponding values in the smooth-wall surface layer were small near the top of a pine forest and would increase with increasing height to approach the value of unity.

The canopy scaling is believed to be valid for moderately dense to very dense canopies. For flow over a spare forest, additional scales such as distance among trees may be needed to capture the influence of individual roughness elements. In this case, the profile model of Garratt (1980) should be considered.

4) OTHER FORMULATIONS

The buoyancy length scale can be defined for stably stratified air as

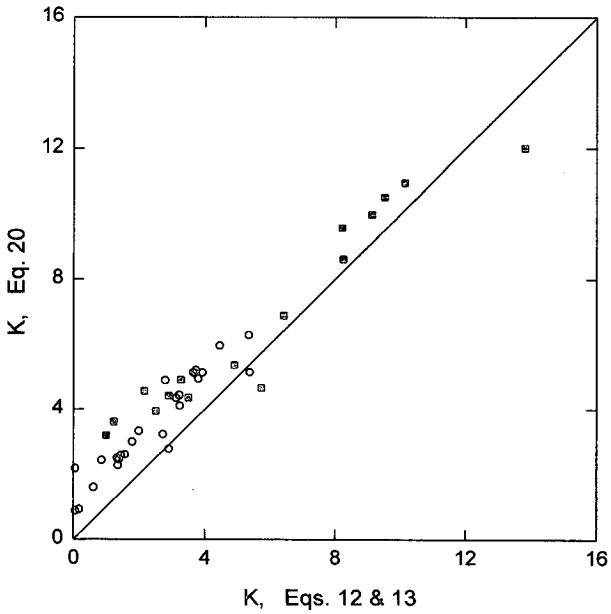

FIG. 9. Comparison of eddy diffusivity ($m^2\ s^{-1}$) calculated from Eq. (12) and (13) ($c = 0.41$) with that from Eq. (20) ($\alpha = 0.27$) for $|\xi| < 0.06$ at CB: solid square, $z = 34.5$ m; open circle, $z = 22.4$ m; line, 1:1.

$$l_b = \frac{\sigma_w}{N}, \tag{23}$$

where N is the Brunt–Väisälä frequency. In general N evolves very slowly with time and can be regarded as an external parameter that regulates the interaction between turbulence and wavelike motions. The scale l_b is understood as the maximum distance within which the vertical displacement of a fluid element is constrained (Pearson et al. 1983; Britter et al. 1983; Hunt et al. 1985), and is generally much larger than l_w. The Lagrangian model of Pearson et al. (1983) suggests

$$K = c_1 l_b \sigma_w. \tag{24}$$

Model simulations (Nieuwstadt 1984; Derbyshire 1995; Schumann and Gerz 1995; Mason and Derbyshire 1990) suggest that c_1 is a stability dependent parameter, its value falling in the range of 0.0–0.3. The observation at the Boulder Atmospheric Observatory yielded a mean value of 0.17, with essentially no trend with stability (Hunt et al. 1985).

Another eddy diffusivity formulation involves the Ozmidov length scale l_O and a buoyancy velocity scale v_b defined as

$$l_O = \left(\frac{\epsilon}{N^3}\right)^{1/2}, \tag{25}$$

$$v_b = \left(\frac{\epsilon}{N}\right)^{1/2}. \tag{26}$$

The eddy diffusivity is thought to be proportional to the product of these two scales (Schumann and Gerz 1995; Osborne 1980)

$$K = c_2 l_O v_b, = \frac{c_2 \epsilon}{N^2}. \tag{27}$$

The average values of the three length scales at z = 34.5 m at CB were (standard deviation in parentheses): l_w = 7.0 (2.2), l_b = 13.6 (9.5) and l_O = 19.9 (18.2) m. The relative magnitudes reported here are typical for a stably stratified fluid.

In Fig. 11 we plot c_1 and c_2 as a function of local air stability ξ. Most data points appear to follow the relations inferred from the MOS functions and Nieuwstadt's theory for flow over smooth surfaces. Assuming that turbulent transport of TKE is negligible in a stable fluid, Osborne (1980) showed that c_2 is constrained by a critical flux Richardson number to lie below 0.2. The maximum observed value of c_2 at CB is 0.55, which would yield an unusually high critical Richardson number of 1.2 if we were to use his formula relating c_2 to the critical Richardson number. Clearly the assumption of negligible turbulent transport is not valid over forests. The average value of c_1 in this plot is 0.24, slightly higher than that of Hunt et al. (1985), while the average value of c_2 is 0.17, which is in close agreement with the finding of Schumann and Gerz (0.14, 1995), who argued that the variation of c_2 is not large for the gradient Richardson number in the range 0.1–0.5.

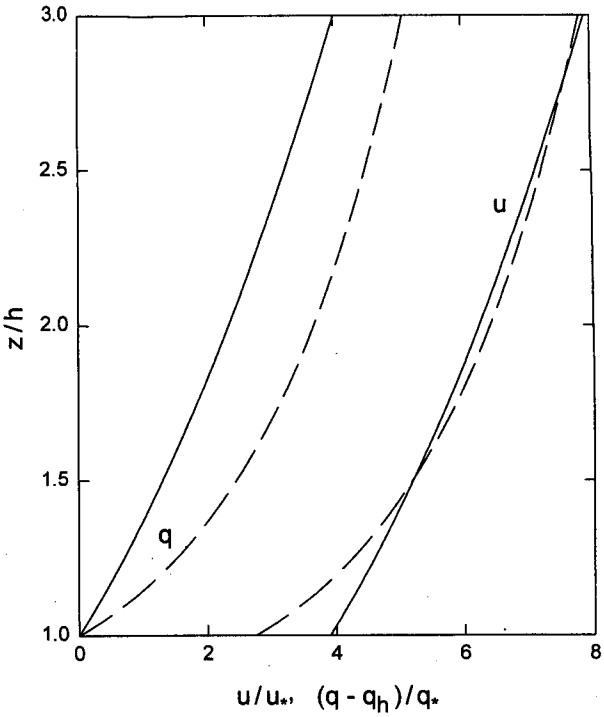

FIG. 10. Profiles of wind speed and scalar concentration over a forest under neutral stability: solid line, Eqs. (21) and (22) (a = 3.20, b = 1.22, α = 0.27); dashed line, logarithmic relations with a displacement height $0.7h$ and a roughness length $0.1h$.

4. Conclusions

Under neutral and unstable conditions the nondimensional dissipation rate of turbulent kinetic energy over the forests is lower than that from its MOS function for the smooth-wall surface layer. The agreement is somewhat better under stable conditions but a large scatter is evident. When the frequency is made nondimensional by h and u_h, the Kaimal spectral model for neutral air describes the observations very well. Data of the vertical velocity spectral maximum suggest that the w spectral curve is more sharply peaked under all stability conditions in comparison to the smooth-wall counterpart. The vertical integral scale shows a rapid increase with increasing instability. The analysis points out that parameters of the canopy scaling (h and u_h) are important scaling dimensions in attempts to formulate quantitative relations for turbulence over forests. Several new nondimensional groups have been introduced, but unlike the MOS theory, which relies solely on dimensional analysis, the present study forms these groups on the basis of physical reasoning.

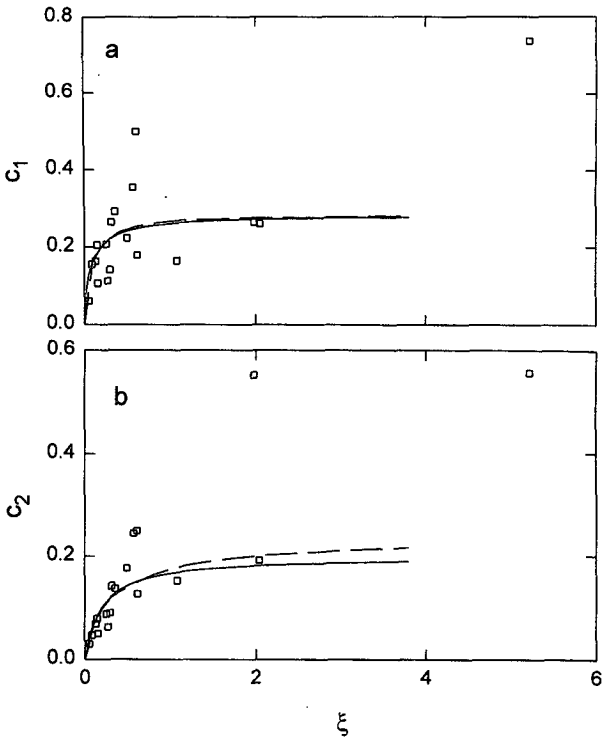

FIG. 11. Coefficients c_1 in Eq. (24) (a) and c_2 in Eq. (27) (b) as a function of air stability: square, observation at z = 34.5 m at CB; solid line, from MOS functions for flow over smooth surfaces; dashed line, from local similarity of Nieuwstadt (1984).

Equation (12), which was first proposed by Hanna (1968) and completely avoids empirical MOS functions, is shown to be a promising way of deriving the eddy diffusivity of sensible heat and other scalars over forests from knowledge of air turbulence. A value of 0.43 was obtained for the proportionality coefficient c for neutral and stable air, which appears to be invariant with ξ for $\xi > 0$. This value is in close agreement with that for the smooth-wall surface layer, indicating that c is a conservative parameter insensitive to surface roughness as well. It is postulated that c is also a conservative parameter for unstable air, its value probably falling between 0.41 and 0.54, although admittedly no data are available at present to allow a direct confirmation.

Profiles of wind speed and the scalar concentration have been derived for neutral air in the roughness sublayer. It is possible that in the absence of ϵ data, local wind speed and air stability can be used to estimate the eddy diffusivity.

The MOS stability parameter ξ has been retained throughout the analysis. However, this parameter is not interpreted as a ratio of two independent vertical dimensions; rather it is understood as the relative balance between the buoyancy production (and destruction in the case of stable conditions) and the shear production of turbulence [term 2 and term 1, respectively, on the rhs of Eq. (5)]. One may wish to modify it by using Eq. (21) to find the velocity shear in the roughness sublayer and obtain a refined stability parameter that depends on h and turbulence intensity as well as momentum and sensible heat fluxes. It remains to be seen whether the refinement will bring any further improvement to the results. Future studies should also consider use of the gradient Richardson number, which is a key parameter in stably stratified shear flow.

Acknowledgments. The author would like to thank Drs. T. A. Black, G. den Hartog, and H. H. Neumann, without whose participation in the field experiments this work would not have been possible. The work is supported by a start-up grant from the School of Forestry and Environmental Studies, Yale University.

APPENDIX

Determining TKE Dissipation from Velocity Derivative with Sonic Anemometers

It can be shown that

$$\overline{\left(\frac{du'}{dx}\right)^2} = \frac{D_{uu}(d)}{d^2}, \tag{A1}$$

where u' is the fluctuating u component measured with a sonic anemometer and D_{uu} is the u structure parameter, which has the following form in the inertial subrange

$$D_{uu} = C_v^2 d^{2/3}. \tag{A2}$$

The proportionality coefficient C_v^2 can be related to TKE dissipation rate via the velocity spectrum in the inertial subrange

$$\begin{aligned} S_u &= 0.25 C_v^2 k_1^{-5/3} \\ &= (2\pi)^{2/3} \alpha_u \epsilon^{2/3} k_1^{-5/3}, \end{aligned} \tag{A3}$$

where k_1 is wavenumber (Tatarskii 1971). Taylor's hypothesis of frozen turbulence is employed to relate spatial derivative to time derivative, as

$$\frac{du'}{dx} \approx \frac{\Delta u'}{u \Delta t}, \tag{A4}$$

where $\Delta u'$ is the difference in u' between two adjacent sampling points and Δt sampling interval. To ensure accuracy of Eq. (A4), it is required that $u\Delta t$ be comparable to the Kolmogorov length scale (e.g., Antonia et al. 1980). Combining Eqs. (A1)–(A4) and solving for ϵ, we have

$$\epsilon = \frac{1}{2\pi} \left(\frac{0.25}{\alpha_u}\right)^{3/2} \left(\frac{d^2}{u^3}\right) \left[\overline{\left(\frac{\Delta u'}{\Delta t}\right)^2}\right]^{3/2}. \tag{A5}$$

REFERENCES

Amiro, B. D., and P. A. Davis, 1988: Statistics of atmospheric turbulence within a natural black spruce forest canopy. *Bound.-Layer Meteor.*, **44,** 267–283.

Anderson, D. E., S. B. Verma, R. J. Clement, D. D. Baldocchi, and D. R. Matt, 1986: Turbulence spectra of CO_2, water vapor, temperature and velocity over a deciduous forest. *Agric. For. Meteor.*, **38,** 81–99.

Antonia, R. A., A. J. Chambers, and N. Phan-Thien, 1980: Taylor's hypothesis and spectra of velocity and temperature derivatives in a turbulent shear flow. *Bound.-Layer Meteor.*, **19,** 19–29.

Britter, R. E., J. C. R. Hunt, L. Marsh, and W. H. Snyder, 1983: Turbulent diffusion in a stratified fluid. *J. Fluid Mech.*, **127,** 27–44.

Businger, J. A., J. C. Wyngaard, Y. Izumi, and E. F. Bradley, 1971: Flux-profile relationships in the atmospheric surface layer. *J. Atmos. Sci.*, **28,** 181–189.

Chen, F., and P. Schwerdtfeger, 1989: Flux-gradient relationships for momentum and heat over a rough natural surface. *Quart. J. Roy. Meteor. Soc.*, **115,** 335–352.

Derbyshire, S. H., 1995: Stable boundary layers: Observations, models and variability. Part I: Modelling and measurements. *Bound.-Layer. Meteor.*, **74,** 19–54.

Dyer, A. J., 1974: A review of flux-profile relationships. *Bound.-Layer Meteor.*, **7,** 363–372.

Fitzjarrald, D. R., B. L. Stormwind, G. Fisch, and O. M. R. Cabral, 1988: Turbulent transport observed just above the Amazon forest. *J. Geophys. Res.*, **93,** 1551–1563.

Gardiner, B. A., 1994: Wind and wind forces in a plantation spruce forest. *Bound.-Layer Meteor.*, **67,** 161–186.

Garratt, J. R., 1980: Surface influence upon vertical profiles in the atmospheric near-surface layer. *Quart. J. Roy. Meteor. Soc.*, **106,** 803–819.

Hanna, S. R., 1968: A method of estimating vertical eddy transport in the planetary boundary layer using characteristics of the vertical velocity spectrum. *J. Atmos. Sci.*, **25,** 1026–1033.

Hill, R. J., 1989: Implications of Monin–Obukhov similarity theory for scalar quantities. *J. Atmos. Sci.*, **46,** 2236–2244.

Högström, U., 1990: Analysis of turbulent structure in the surface layer with a modified similarity formulation for near neutral conditions. *J. Atmos. Sci.*, **47,** 1949–1972.

——, H. Bergström, A. Smedman, S. Halldin, and A. Lindroth, 1989: Turbulent exchange above a pone forest. Part I: Fluxes and gradients. *Bound.-Layer Meteor.*, **49,** 197–217.

Hunt, J. C. R., J. C. Kaimal, and J. E. Gaynor, 1985: Some observations of turbulence structure in stable layers. *Quart. J. Roy. Meteor. Soc.*, **111,** 793–815.

Kaimal, J. C., and J. J. Finnigan, 1994: *Atmospheric Boundary Layer Flows: Their Structure and Measurement,* Oxford University Press, 289 pp.

——, J. C. Wyngaard, and D. A. Haugen, 1968: Deriving power spectra from a three-component sonic anemometer. *J. Appl. Meteor.*, **7,** 827–837.

——, ——, Y. Izumi, and O. R. Coté, 1972: Spectral characteristics of surface layer turbulence. *Quart. J. Roy. Meteor. Soc.*, **98,** 563–589.

Kristensen, L., and D. R. Fitzjarrald, 1984: The effect of line averaging on scalar flux measurements with a sonic anemometer near the surface. *J. Atmos. Oceanic Technol.*, **1,** 138–146.

Leclerc, M. Y., K. C. Beissner, R. H. Shaw, G. den Hartog, and H. H. Neumann, 1990: The influence of atmospheric stability on the budgets of the Reynolds stress and turbulent kinetic energy within and above a deciduous forest. *J. Appl. Meteor.*, **29,** 916–933.

Lee, X., and T. A. Black, 1993: Atmospheric turbulence within and above a Douglas-fir stand. Part I: Statistical properties of the velocity field. *Bound.-Layer Meteor.*, **64,** 149–174.

——, ——, G. den Hartog, H. H. Neumann, Z. Nesic, and J. Olejnik, 1996: Carbon dioxide exchange and nocturnal processes over a mixed deciduous forest. *Agric. For. Meteor.*, in press.

Mason, P. J., and S. H. Derbyshire, 1990: Large-eddy simulation of the stably-stratified atmosphere boundary layer. *Bound.-Layer Meteor.*, **53,** 117–162.

Meyers, T. P., and D. D. Baldocchi, 1991: The budget of turbulent kinetic energy and Reynolds stress within and above a deciduous forest. *Agric. For. Meteor.*, **53,** 207–222.

Neumann, H. H., G. den Hartog, and R. H. Shaw, 1989: Leaf area measurements based on hemispheric photographs and leaf-litter collection in a deciduous forest during autumn leaf-fall. *Agric. For. Meteor.*, **45,** 325–345.

Nieuwstadt, F. T. M., 1984: The turbulent structure of the stable nocturnal boundary layer. *J. Atmos. Sci.*, **41,** 2202–2216.

Osborne, T. R., 1980: Estimates of the local rate of vertical diffusion from dissipation measurements. *J. Phys. Oceanogr.*, **10,** 83–89.

Panofsky, H. A., and J. A. Dutton, 1984: *Atmospheric Turbulence: Models and Methods for Engineering Applications,* John Wiley and Sons, 397 pp.

——, H. Tennekes, D. H. Lenschow, and J. C. Wyngaard, 1977: The characteristics of turbulent velocity components in the surface layer under convective conditions. *Bound.-Layer Meteor.*, **11,** 355–361.

Paw U, K. T., Y. Brunet, S. Collineau, R. H. Shaw, T. Maitani, J. Qiu, and L. Hipps, 1992: On coherent structures in turbulence above and within agricultural plant canopies. *Agric. For. Meteor.*, **61,** 55–68.

Pearson, H. J., J. S. Puttock, and J. C. R. Hunt, 1983: A statistical model of fluid element motions and vertical diffusion in homogeneous stratified fluid. *J. Fluid Mech.*, **129,** 219–249.

Raupach, M. R., P. A. Coppin, and B. J. Legg, 1986: Experiments on scalar dispersion within a model plant canopy. Part I: The turbulence structure. *Bound.-Layer Meteor.*, **35,** 21–52.

——, J. J. Finnigan, and Y. Brunet, 1989: Coherent eddies in vegetation canopies. *Fourth Australasian Conf. on Heat and Mass Transfer,* Christchurch, New Zealand, 75–90.

Schumann, U., and T. Gerz, 1995: Turbulent mixing in stably stratified shear flows. *J. Appl. Meteor.*, **34,** 33–48.

Shaw, R. H., R. H. Silversides, and G. W. Thurtell, 1974: Some observations of turbulence and turbulent transport within and above plant canopies. *Bound.-Layer Meteor.*, **5,** 429–449.

——, G. den Hartog, and H. H. Neumann, 1988: Influence of foliar density and thermal stability on profiles of Reynolds stress and turbulence intensity in a deciduous forest. *Bound.-Layer Meteor.*, **45,** 391–409.

Silverman, B. A., 1968: The effect of spatial averaging on spectrum estimation. *J. Appl. Meteor.*, **7,** 168–172.

Stull, R. B., 1988: *An Introduction to Boundary Layer Meteorology.* Kluwer Academic Press, 666 pp.

Tanner, C. B., and G. W. Thurtell, 1969: Anemoclinometer measurements of Reynolds stress and heat transport in the atmospheric surface layer. Research and Development Tech. Rep. ECOM-66-G22F, University of Wisconsin, Madison, WI, 10 pp.

Tatarskii, V. I., 1971: *The Effects of the Turbulent Atmosphere on Wave Propagation.* Kefer, 472 pp.

Tennekes, H., and J. L. Lumley, 1972: *A First Course in Turbulence.* MIT Press, 300 pp.

Thompson, N., 1979: Turbulence measurements above a pine forest. *Bound.-Layer Meteor.*, **16,** 293–310.

Wilson, J. D., D. P. Ward, G. W. Thurtell, and G. E. Kidd, 1982: Statistics of atmospheric turbulence within and above a corn canopy. *Bound.-Layer Meteor.*, **24,** 495–519.

Wilson, R. N., and R. H. Shaw, 1977: A higher order closure model for canopy flow. *J. Appl. Meteor.*, **16,** 1197–1205.

Wyngaard, J. C., and O. R. Coté, 1971: The budgets of turbulent kinetic energy and temperature variance in the atmospheric surface layer. *J. Atmos. Sci.*, **28,** 190–201.